

## Assessing the effectiveness of a NSM-CFRP flexural strengthening technique for continuous RC slabs by experimental research

Gláucia Dalfré and Joaquim Barros

ISISE – University of Minho, Guimarães, Portugal

**ABSTRACT:** This work reports the results of an ongoing investigation on the use of the Near Surface Mounted (NSM) CFRP laminates for the flexural strengthening of continuous Reinforced Concrete (RC) slabs, in order to verify the possibility of increasing the negative resisting bending moment in 25%, maintaining moment redistribution levels of about 30%. To better understand the behavior of these structures, a comprehensive experimental program was proposed with the aim of evaluating the possibilities of NSM technique for statically indeterminate RC slab strips in terms of flexural strengthening effectiveness, moment redistribution and ductility performance. To assess the behavior of the tested slab strips the strains in CFRP laminates, steel reinforcement and concrete surfaces, as well as the applied load and support reactions were registered up to failure of the slabs. The experimental program is described and the obtained results are presented and analyzed in this paper.

### 1 INTRODUCTION

In general, when a structural Reinforced Concrete (RC) element is strengthened with fiber reinforced polymer (FRP) systems, its failure mode tends to be more brittle than its unstrengthened homologous element, due to the intrinsic bond conditions between these systems and the concrete substrata, as well as the linear-elastic brittle tensile behavior of FRPs. In case of continuous RC slabs and beams (statically indeterminate structures), the use of FRP systems to increase their flexural resistance can even compromise the moment redistribution capacity of these types of elements.

Although many in situ RC elements are of continuous construction, there is a lack of experimental and theoretical studies in the behavior of statically indeterminate RC members strengthened with FRP materials. Park and Oehlers (2000) performed tests on continuous beams with externally bonded steel or FRP reinforcement over the sagging and hogging regions. Due to the geometry of the beams and the test set-up, almost zero moment redistribution was obtained in all the tests. El-Refaie et al. (2003) and Ashour et al. (2004) tested continuous beams strengthened in flexure with externally bonded CFRP sheets or plates over the hogging and/or sagging regions, with different arrangements of internal steel reinforcement. As a result, all the strengthened beams exhibited a higher beam load capacity but lower ductility compared with their respective unstrengthened control beams. Oehlers et al. (2004) carried out tests on seven continuous beams of two spans strengthened by adhesively bonding FRP or metal plates only in the hogging region. The steel reinforcing arrangement adopted in the hogging was designed to ensure that the hogging region reaches its moment capacity first. All of the beams presented, at least, a moment redistribution capacity of 20% before debonding, and five beams had a moment redistribution level greater than the upper limit of 30% recommended by international standards.

Tests with simply supported RC members strengthened with NSM have shown that NSM debonds or fails at much higher strain than EBR strengthening, therefore, in general, NSM strengthened members are expected to have a much more ductile behavior than EBR strengthened members. However, limited information is available in literature dealing with the behavior of continuous structures strengthened according to the NSM technique. In this context, nine continuous beams of two-spans, strengthened in the hogging region according to the NSM technique, were tested to determine the ductility capacity of these strengthened beams (Liu 2005; Liu et al 2006). The results showed that the beams strengthened with NSM steel and NSM CFRP laminates achieved a moment redistribution percentage of 39% and 32%, respectively. Additionally, it was found that the debonding strains when using NSM technique were considerably larger than those associated with EB plates, which justifies the relatively high moment redistribution levels observed in the NSM strengthened beams.

Bonaldo (2008) carried out an experimental program to analyze the moment redistribution capability of two-span continuous RC slabs strengthened according to the NSM technique. The experimental program was composed of three series of three slab strips of two equal span length, in order to verify the possibility of maintaining moment redistribution levels of 15%, 30% and 45% when the flexural resistance of the intermediate support region is increased in 25% and 50%. Though the flexural resistance of the NSM strengthened sections has exceeded the target values, the moment redistribution was relatively low, and the increase of the load carrying capacity of the strengthened slabs did not exceed 25%. This experimental program was recently analyzed to highlight the possibilities of NSM technique for statically indeterminate RC slabs in terms of flexural strengthening effectiveness, moment redistribution and ductility performance. Using a FEM-based computer program, a high effective NSM flexural strengthening strategy was proposed, capable of enhancing the slab's load carrying capacity and maintaining high levels of ductility (Dalfré and Barros, 2010). Thus, these results suggest that the NSM technique can be used to increase the load carrying capacity of RC structures with little, if any, loss of ductility.

In the present paper the potentialities of the NSM technique is explored for the increase of the load carrying capacity of two spans continuous RC slabs. The NSM strengthening configurations applied in the slab strip were designed to increase in 25% the load carrying capacity of its corresponding unstrengthened control RC slab. Besides the load carrying capacity of the tested slabs, the moment redistribution issue is discussed in this paper.

## 2 EXPERIMENTAL PROGRAM

### 2.1 *Specimen and Test Configuration*

The experimental program is composed by the two RC slab strips with the geometry, support and load conditions, reinforcement and strengthening arrangements represented in Figure 1. The steel reinforcement arrangements in the reference slab (with the designation of SL30) were designed for a load of 46.2 kN, which is the load that introduces a deflection of  $L/480$  ( $L=2800$  mm is the span length of the slab) recommended by the ACI 318 (2004), and assuming a moment redistribution of 30%. Furthermore, in the evaluation of these reinforcement arrangements a strain limit of 3.5‰ for the concrete crushing was assumed.

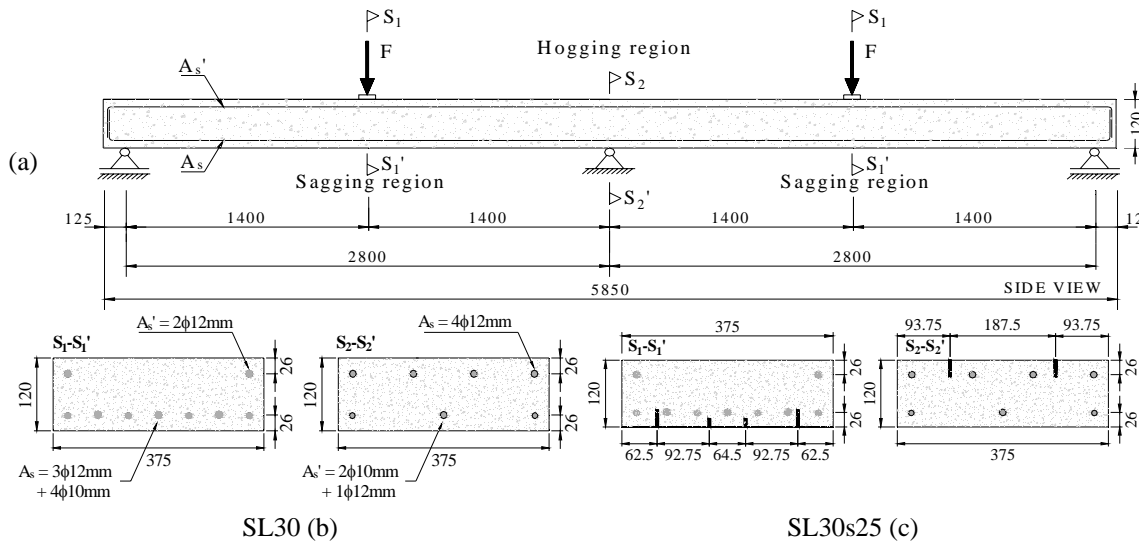


Figure 1. Slab strips: (a) test configuration, (b and c) cross-sectional dimensions at sagging (S1-S1') and hogging regions (S2-S2'). All dimensions are in mm.

According to the CEB-FIB Model Code (1993), the coefficient of moment redistribution,  $\delta = M_{red}/M_{elas}$ , is defined as the relationship between the moment in the critical section after redistribution ( $M_{red}$ ) and the elastic moment ( $M_{elas}$ ) in the same section calculated according to the theory of elasticity, while  $\eta = (1 - \delta) \cdot 100$  is the moment redistribution percentage. The NSM flexural strengthened slab has the same steel reinforcement arrangement adopted in the reference slab, and a number of CFRP laminates applied in the hogging (intermediate support) and sagging regions (loaded zones) designed in order to increase the load carrying capacity of the reference slab (REF) in 25%.

The design of cross sections subject to flexure was based on stress and strain compatibility, where the maximum strain at extreme concrete compression fiber was assumed equal to 0.0035. To increase the load carrying capacity in 25% the strengthening arrangement represented in Figure 1(c) was adopted. In the hogging region, two  $1.4 \times 20 \text{ mm}^2$  cross section area CFRP laminates were applied, while in both sagging regions two  $1.4 \times 20 \text{ mm}^2$  and two  $1.4 \times 10 \text{ mm}^2$  CFRP laminates were installed. This slab has the designation of SL30s25.

The test with the strengthened slab strip had two phases. In the first phase the slab was loaded up to attain in the loaded sections a deflection corresponding to 50% of the deflection measured in the reference slab when steel reinforcement in the hogging region (H) has attained its yield strain. When attained this deflection level (5.80 mm), a temporary reaction system was applied to maintain this deformability during the period necessary to strengthen the slab. To control the maintenance of this deflection, dial gauges were used to adjust the temporary reaction system when necessary. Therefore, the strengthening process was applied maintaining the slab with a damage level that can be representative of real slabs requiring structural rehabilitation. After the curing time of the adhesives used to bond the NSM CFRP strips (which in general took about two weeks), the temporary reaction system was removed, while the load was transferred to the slab. This stress transfer process was governed by the criteria of maintaining the deflection level that corresponds to the initiation of the second phase of the test (5.80 mm). This second phase ended when the strengthened slab strip has ruptured.

## 2.2 Measuring Devices

Figure2 depicts the positioning of the sensors for data acquisition in the tests. To measure the vertical deflection of a slab strip, six linear voltage differential transducers (LVDT 82803, LVDT 60541, LVDT 82804, LVDT 19906, LVDT 18897 and LVDT 3468) were supported in a suspension bar (Figure 2a). The LVDTs 60541 and 18897, placed at the slab loaded sections, were also used to control the test at a displacement rate of 10  $\mu\text{m/s}$  up to the deflection of 50 mm. After this deflection, the internal LVDTs of the actuators were used to control the test at a displacement rate of 20  $\mu\text{m/s}$  up to the failure of the slab strip. The force ( $F_{(522)}$ ) applied at the left span (Figure2a) was measured using a load cell of  $\pm 200$  kN and accuracy of  $\pm 0.03\%$  (designated Ctrl\_1), placed between the loading steel frame and the actuator of 150 kN load capacity and 200 mm range. In the right span, the load ( $F_{(123)}$ ) was applied with an actuator of 100 kN and 200 mm range, and the corresponding force was measured using a load cell of  $\pm 250$  kN and accuracy of  $\pm 0.05\%$  (designated Ctrl\_2). To monitor the reaction forces, load cells were installed under two supports. One load cell (AEP\_200) was positioned at the central support (nonadjustable support), placed between the reaction steel frame and the slab's support device (Figure2a). The other load cell (MIC\_200) was positioned in-between the reaction steel frame and the apparatus of the adjustable right support of the slab. These cells have a load capacity of 200 kN and accuracy of  $\pm 0.05\%$ . To monitor the strain variation in the steel bars, concrete and CFRP laminates, the arrangements of strain gauges (SGs) represented in Figure2(b-e) were adopted. Eleven SGs were installed in steel bars, seven of them in steel bars at top surface in the hogging region (SG1 to SG7) and the other four in steel bars at bottom surface in the sagging regions (SG8 to SG11, Figure2b-c). Six SGs were applied at the external concrete surface in the compression regions (SG12 to SG17, Figure2d). Finally, three SGs (SG18 to SG20) were bonded along one CFRP laminate in the hogging region and three SGs (SG21 to SG23 and SG24 to SG26) were installed along one CFRP laminate in both sagging regions (Figure2e).

## 2.3 Material Properties

At the slabs testing age the average compressive strength and Young's Modulus of the concrete of the SL30 and SL30s25 slabs were (NP-E397, 1993): 30.10 MPa (1.08 MPa), 31.52 GPa (0.86 GPa); 32.59 MPa (1.15 MPa), 30.62 GPa (2.42 GPa), where the values in between round brackets are the corresponding standard deviation. Table 1 includes the values obtained from experimental tests for the characterization of the steel bars and CFRP laminates. For the characterization of the tensile behaviour of the epoxy adhesive, uniaxial tensile tests were performed complying with the procedures outlined in ISO 527-2 (1993), having been obtained an elasticity modulus and a tensile strength of 7.91 GPa [5.16%], and 19.10 MPa [15.59%], respectively, where the values between square brackets correspond to the coefficient of variation.

## 3 MAIN RESULTS OF THE EXPERIMENTAL PROGRAM

Figures 3 to 6 represent relevant results of the experimental program. Table 2 resumes the results obtained numerically for three scenarios: (i) when a plastic hinge formed at the hogging region (superscript H) and at the sagging regions (superscript S), (ii) when the maximum concrete compressive strain attained 3.5 ‰ (symbols with subscript "cu") in the hogging and sagging regions ( $\varepsilon_{c,\max} = 3.5\text{‰}$ , which is assumed the concrete crushing strain) and (iii) at  $\bar{F}_{\max}$ .

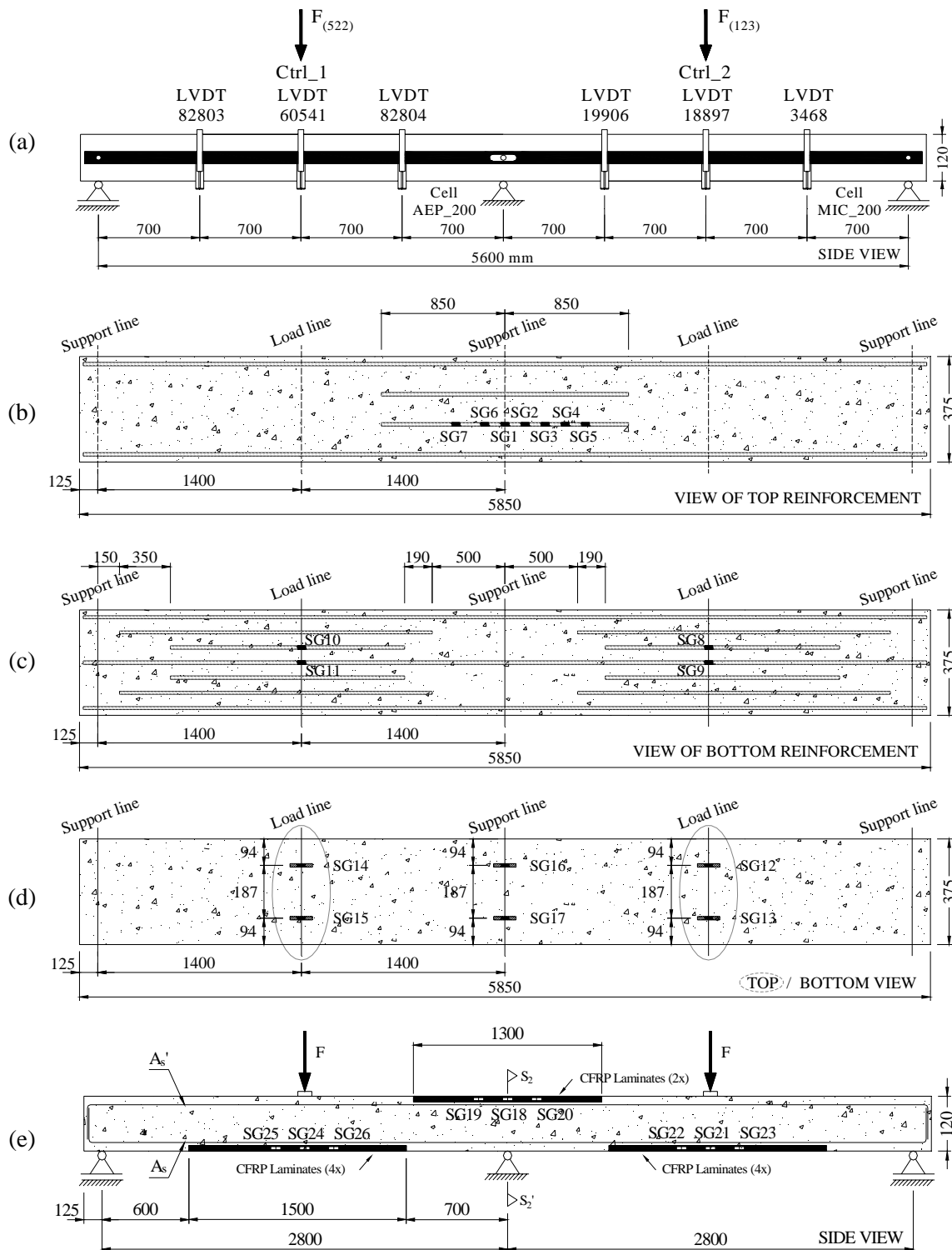


Figure 2. Arrangement of displacement transducers and strain gauges: (a) displacement transducers; layout of strain gauges at steel bars at hogging (b) and sagging (c) region; (d) strain gauges at concrete slab surfaces, (e) layout of strain gauges at CFRP laminates for SL30s25 (all dimensions are in mm).

Table 1. Summary of the properties of steel reinforcement and CFRP laminates.

Steel reinforcement					CFRP Laminate			
Steel bar diameter ( $\phi_s$ )	Modulus of Elasticity (GPa)	Yield stress (0.2 %) <sup>a</sup> (MPa)	Strain at yield stress <sup>b</sup>	Tensile strength (MPa)	CFRP laminate height	Ultimate tensile stress <sup>c</sup> (MPa)	Ultimate tensile strain <sup>c</sup> (%)	Modulus of Elasticity (GPa)
10 mm	178.24 (2.48%)	446.95 (3.25%)	0.0027 (0.45%)	575.95 (0.34%)	10 mm	2867.63 (3.07%)	17.67 (3.04%)	159.30 (3.15%)
12 mm	198.36 (2.77%)	442.47 (2.87%)	0.0024 (0.19%)	539.88 (1.84%)	20 mm	2782.86 (2.73%)	17.76 (3.13%)	156.69 (0.73%)

<sup>a</sup>Yield stress determined by the “Offset Method”, according to ASTM A370 (2002); <sup>b</sup>Strain at yield point, for the 0.2 % offset stress; (value) Coefficient of Variation (COV) = (Standard deviation/Average) x 100; <sup>c</sup>Uniaxial tensile tests carried out according to ISO 527-1 (1993) and ISO 527-5 (1993) recommendations.

In this Table,  $F_y^H$  and  $F_y^S$  are the loads at the formation of the plastic hinge at hogging and sagging regions, respectively,  $u_y^H$  and  $u_y^S$  are the average deflection for  $F_y^H$  and  $F_y^S$ , respectively,  $\epsilon_c^H$  and  $\epsilon_c^S$  are the maximum concrete strains registered at H and S regions,  $\epsilon_s^H$  and  $\epsilon_s^S$  are the maximum strains in steel bars at H and S regions, respectively, and, finally,  $\epsilon_f^H$  and  $\epsilon_f^S$  are the maximum strains in the CFRP laminates at H and S regions. Additionally,  $\bar{F}_{max}$  is the maximum average load ( $\bar{F}_{max} = (F_{(522)} + F_{(123)})/2$ ),  $R_{L, \bar{F}_{max}}$  is the load registered at the load cell (MIC\_200) and  $\Delta \bar{F}_{max} / \bar{F}_{max}^{REF}$  is the increase in terms of load carrying capacity provided by the strengthening technique at  $\bar{F}_{max}$ .  $\eta$  is the moment redistribution percentage for  $F_y^H$ ,  $F_y^S$ ,  $F_{cu}^H$ ,  $F_{cu}^S$  and  $\bar{F}_{max}$ .

From the analysis of the results it can be outlined the following: 1) For a compressive strain of 3.5 ‰, the increase of the load carrying capacity provided by the strengthening system was of about 29 %; 2) Up to the formation of the plastic hinges the strains in the laminates ranged from 1.13‰ to 6.72‰; 3) The contribution of the CFRP laminates was limited by the premature failure mode by the detachment of the concrete cover layer that includes the laminates at the hogging region; 4) The moment redistribution percentage at  $F_{cu}^S$  and  $\bar{F}_{max}$  was 21% and 27% for the SL30s25, which are lower than the target limit, but still quite high values.

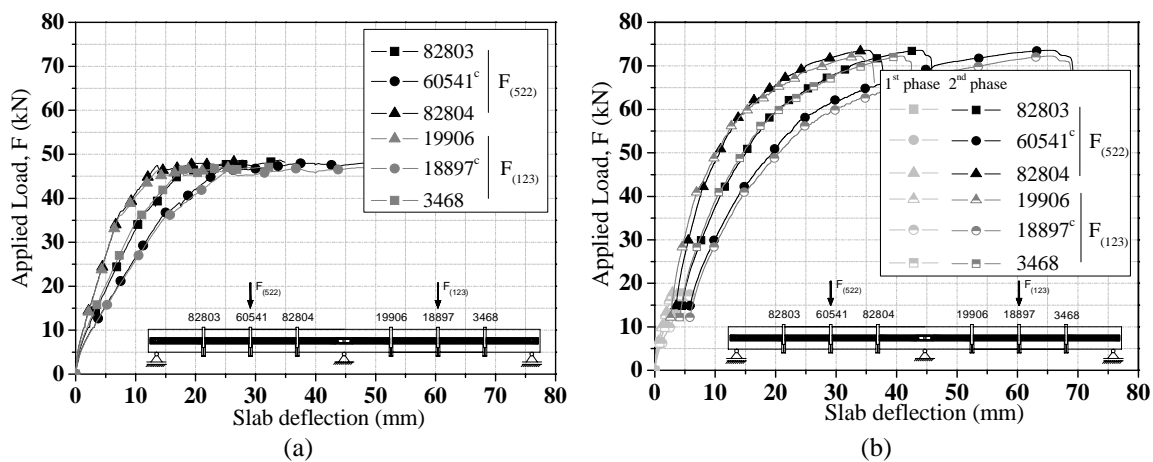


Figure 3. Load-deflection curves: (a) SL30 and (b) SL30s25.

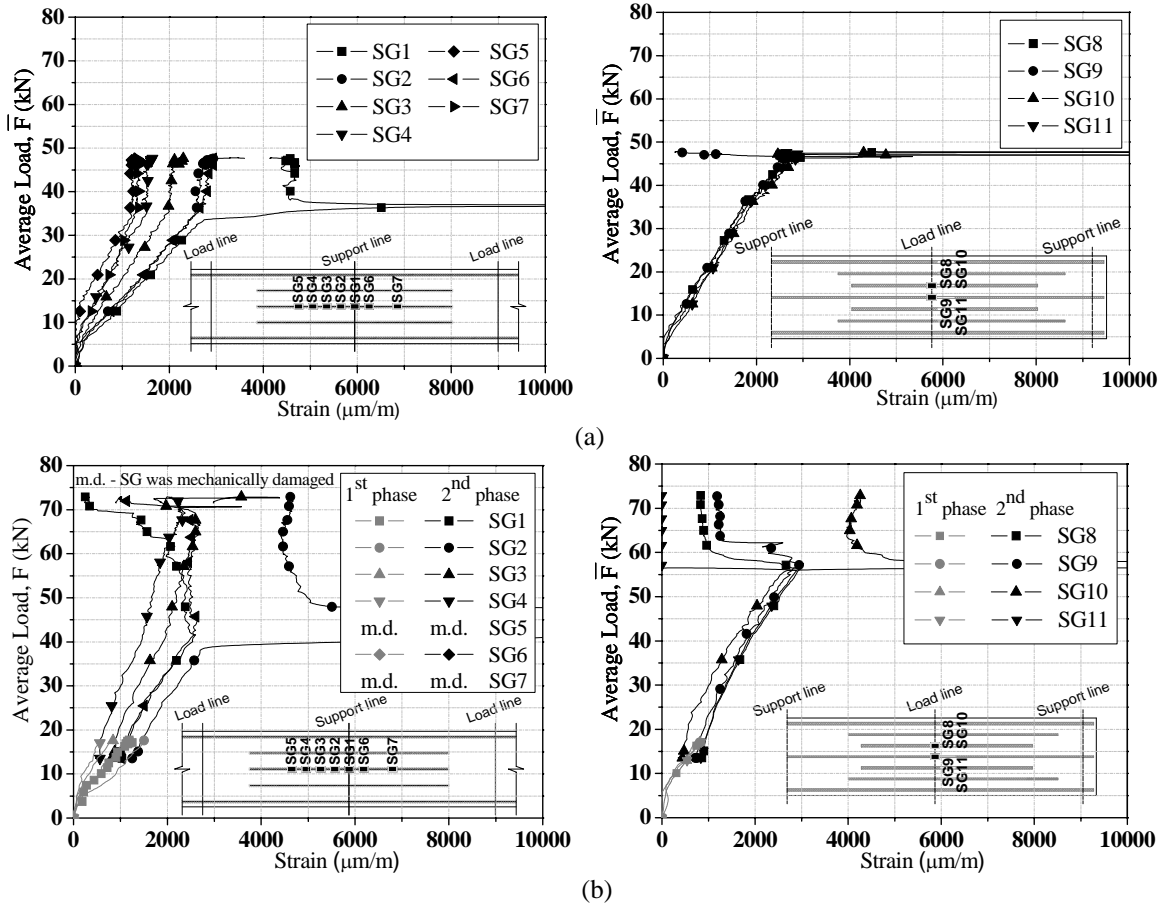


Figure 4. Load –strain relationships in steel: (a) SL30 and (b) SL30s25.

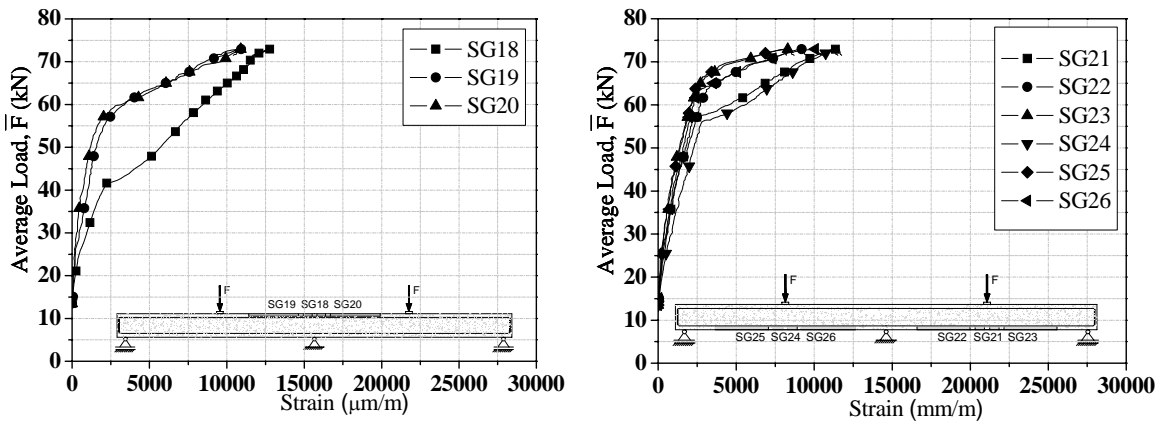


Figure 5. Force –strain relationships in CFRP laminates of SL30s25.

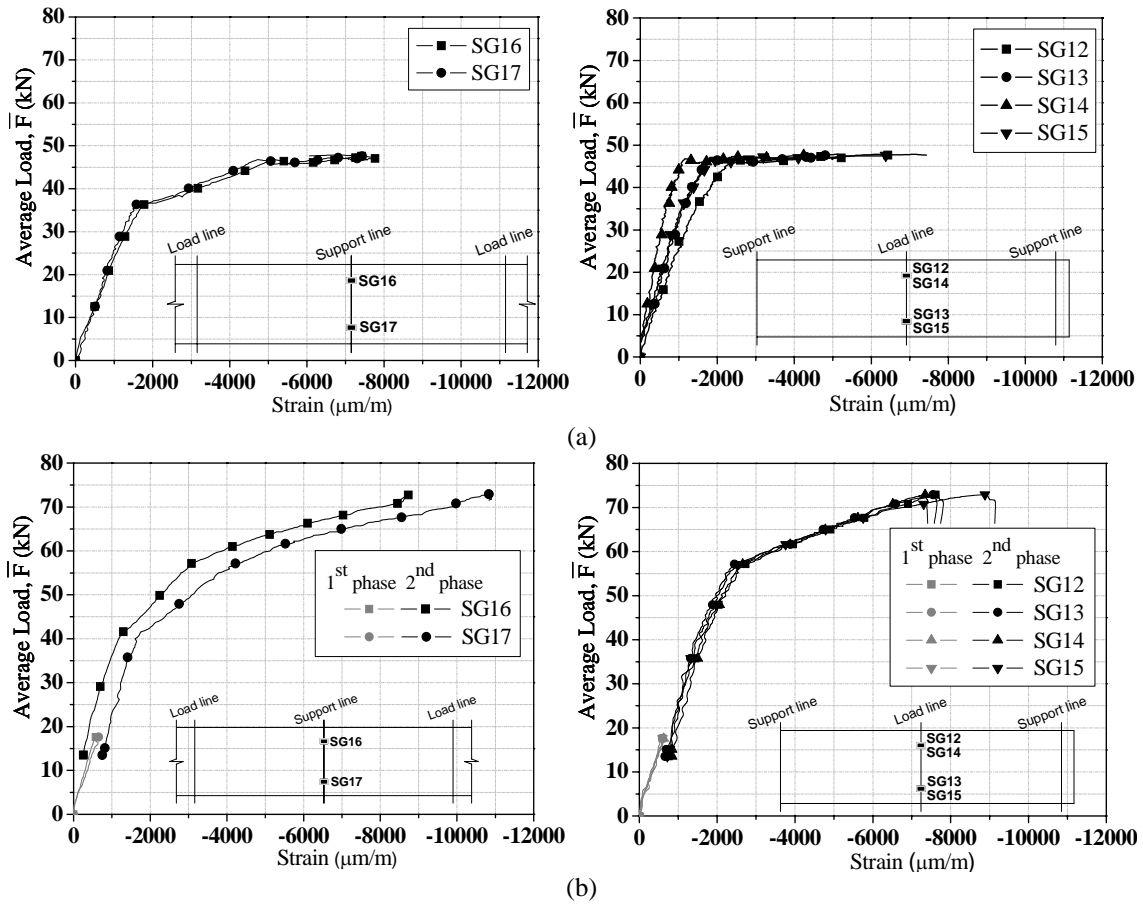


Figure 6. Force –strain relationships in concrete: (a) SL30 and (b) SL30s25.

Table 2. Main results

Slab ID	Hinge at hogging region (H)								Concrete crushing at H					
	$F_y^H$ (kN)	$u_y^H$ (mm)	$\epsilon_c^H$ (‰)	$\epsilon_c^S$ (‰)	$\epsilon_s^S$ (‰)	$\epsilon_s^H$ (‰)	$\epsilon_f^H$ (‰)	$\epsilon_f^S$ (‰)	$F_{cu}^H$ (kN)	$u_{cu}^H$ (mm)	$\epsilon_{s,max}^S$ (‰)	$\epsilon_{s,max}^H$ (‰)	$\epsilon_{f,max}^H$ (‰)	$\epsilon_{f,max}^S$ (‰)
SL30	32.67	13.08	-1.50	-1.30	1.73	2.55	-----	-----	41.27	19.74	2.37	4.47	-----	-----
SL30s25	41.00	14.51	-1.69	-1.69	1.94	2.50	2.15	1.13	53.05	21.87	2.75	2.38	6.51	2.52
Slab ID	Hinge at sagging region (S)								Concrete crushing at S					
	$F_y^S$ (kN)	$u_y^S$ (mm)	$\epsilon_c^H$ (‰)	$\epsilon_c^S$ (‰)	$\epsilon_s^S$ (‰)	$\epsilon_s^H$ (‰)	$\epsilon_f^H$ (‰)	$\epsilon_f^S$ (‰)	$F_{cu}^S$ (kN)	$u_{cu}^S$ (mm)	$\epsilon_{s,max}^S$ (‰)	$\epsilon_{s,max}^H$ (‰)	$\epsilon_{f,max}^H$ (‰)	$\epsilon_{f,max}^S$ (‰)
SL30	41.28	19.74	-3.49	-1.88	2.40	4.47	-----	-----	46.14	30.51	2.84	4.64	-----	-----
SL30s25	53.87	22.41	-3.58	-2.44	2.60	2.45	6.72	2.58	59.91	28.54	4.41	4.43	8.46	5.59
Slab ID	At $\bar{F}_{max}$			$\eta$ (%) at:										
	$\bar{F}_{max}$ (kN)	$R_{L,\bar{F}_{max}}$ (kN)	$\frac{\Delta\bar{F}_{max}}{\bar{F}_{max}^{REF}}$ (%)	$F_y^H$	$F_y^S$	$F_{cu}^H$	$F_{cu}^S$	$\bar{F}_{max}$						
SL30	47.85	16.43	-----	3.38	14.00	14.00	19.94	19.70						
SL30s25	72.96	26.19	52.47	8.27	19.14	18.21	21.45	26.58						



#### 4 CONCLUSIONS

This work deals with the use of the NSM CFRP laminates for the flexural strengthening of continuous RC slabs. The strengthening procedures adopted in the laboratory tests followed, as much as possible, the real strengthening practice for this type of interventions. The obtained results show that the proposed technique is able to increase the load carrying capacity of RC slabs and preserves relevant levels of moment redistribution. The load carrying capacity of the strengthened slab was, however, limited by the detachment of the strengthened concrete cover layer at the intermediate support.

#### 5 ACKNOWLEDGEMENTS

The authors wish to acknowledge the support provided by the S&P® and Secil Companies. The study reported in this paper forms a part of the research program “CUTINEMO - Carbon fiber laminates applied according to the near surface mounted technique to increase the flexural resistance to negative moments of continuous reinforced concrete structures” supported by FCT, PTDC/ECM/73099/2006. The first author would like to acknowledge the National Council for Scientific and Technological Development (CNPq) – Brazil for financial support for scholarship (GDE 200953/2007-9).

#### 6 REFERENCES

- ACI Committee 318. 2004. Building code requirements for structural concrete and Commentary (ACI 318-04). Reported by committee 318, American Concrete Institute, Detroit, 351 pp.
- ASTM A370. 2002. Standard test methods and definitions for mechanical testing of steel products. American Society for Testing and Materials.
- Ashour, A. F.; El-Rafaie; S. A.; Garrity, S. W. 2004. Flexural strengthening of RC continuous beams using CFRP laminates, *Cement and Concrete Composites*, No. 26, pp. 765-775.
- Bonaldo, E.. 2008. Composite materials and discrete steel fibres for the strengthening of thin concrete structures. PhD Thesis, University of Minho, Guimarães, Portugal.
- CEB-FIP Model Code 1990. 1993. “Design Code”. Thomas Telford, Lausanne, Switzerland.
- Dalfré, G. M.; Barros, J. A. O. 2010. Flexural Strengthening of RC Continuous Slab Strips using NSM CFRP Laminates. *Journal of Advances in Structural Engineering* (article accepted for publication)
- El-Refaie, S. A.; Ashour, A. F.; Garrity, S. W. 2003. Sagging and hogging strengthening of continuous reinforced concrete beams using CFRP sheets, *ACI Structural Journal*, Vol. 100, No. 4, pp. 446-453.
- ISO 527-1. 1993. Plastics - Determination of tensile properties - Part 1: General principles. International Organization for Standardization (ISO), Genève, Switzerland, 9 pp.
- ISO 527-2. 1993. Plastics - Determination of Tensile Properties - Part 2: Test Conditions for Moulding and Extrusion Plastics. International Organization for Standardization (ISO), Geneva, Switzerland.
- ISO 527-5. 1993. Plastics - Determination of tensile properties - Part 5: Test conditions for unidirectional fibre-reinforced plastic composites. International Organization for Standardization (ISO), Genève, Switzerland, 9 pp.
- LNEC NP-E397. 1993. Concrete - Assessment of the elasticity modulus under uniaxial compression. Laboratório Nacional de Engenharia Civil, (in Portuguese).
- Liu, I.S.T. 2005. Intermediate crack debonding of plated reinforced concrete beams. PhD Thesis, School of Civil and Environmental Engineering, The University of Adelaide, Adelaide, Australia.
- Liu, IST, Oehlers, DJ, and Seracino, R. 2006. Tests on the ductility of reinforced concrete beams retrofitted with FRP and steel near-surface mounted plates. *Journal of Composites for Construction*, 10(2): 106-114.
- Oehlers, D. J.; Ju, G.; Liu, I. S. T.; Seracino, R. 2004. Moment redistribution in continuous plated RC flexural members. Part 1: neutral axis depth approach and tests, *Engineering Structures*, Vol. 26, No. 14, pp. 2197-2207.
- Park, S. M.; Oehlers, D. J. 2000. Details of tests on steel and FRP plated continuous reinforced concrete beams, School of Civil and Environmental Engineering, University of Adelaide, Research Report R170.